Experimental analysis of different software packages for orientation and digital surface modelling from UAV images

Giovanna Sona · Livio Pinto · Diana Pagliari · Daniele Passoni · Rossana Gini

Received: 6 August 2013 / Accepted: 23 December 2013 / Published online: 15 January 2014

Introduction

Aerial surveys carried out by Unmanned Aerial Vehicles (UAVs) are under quick expansion, thanks to the development of new platforms equipped with automatic systems for plan-ning and controlling the flights and to the improvement of sensors and data acquisition devices.

As a consequence, the increased ease of use widens the employment of UAVs for proximal sensing; the capabilities of these systems are widely explored according to different re-quirements. Some interesting analysis of UAV usage in the close-range field can be found in Remondino et al. (2011), Eisenbeiss and Sauerbier (2011), Colomina et al. (2008). Although it is nowadays clear that unmanned aerial systems are a flexible technology able to collect a big amount of high resolution information, some investigation is still needed to assess the accuracies that such imagery can reach, both for metric and interpretation uses.

G. Sona · R. Gini
Politecnico di Milano, DICA, Via Valleggio, 11, 22100 Como, Italy

G. Sona
e-mail: giovanna.sona@polimi.it

R. Gini
e-mail: rossana.gini@polimi.it

L. Pinto · D. Pagliari (✉) · D. Passoni
Politecnico di Milano, DICA, Piazza Leonardo da Vinci 32,
20133 Milano, Italy
e-mail: diana.pagliari@polimi.it

L. Pinto
e-mail: livio.pinto@polimi.it

D. Passoni
e-mail: daniele.passoni@polimi.it

The limited payload implies the use of new, ultra-light sensors, often less precise with respect to the normal-size ones. Very small digital cameras, for instance, can be used to acquire a large amount of images at very high resolution, but are usually affected by higher deformations compared with photogrammetric calibrated cameras.

Furthermore, new methods for data post-processing are under development, as UAV data can require the use of non-traditional approaches (Grenzdörffer et al. 2008; Haarbrink and Koers 2006; Remondino et al. 2009). As regards aerial images surveys, two different approaches are generally used and tested: digital images taken from UAVs can be processed using traditional photogrammetric methods or software coming from the computer vision (CV) field. In the first case, high accuracy in points coordinates determination and in 3D modelling is the main pursued requirement, whilst the others work mainly to achieve a quick processing and an effective final product.

In the present work, some further tests are presented, performed with the purpose of validating vector-sensor systems and optimizing the UAVs survey for 3D modelling and to compare different software packages that follow different workflows, in order to evaluate their effectiveness and weaknesses.

In this frame, images taken by compact cameras mounted on UAVs are processed by standard photogrammetric software (PhotoModeler, Erdas LPS) and home-made software like EyeDEA developed by University of Parma (Roncella et al. 2011), Calge developed by the Dept. ICA of Politecnico di Milano (Forlani 1986) or by software specifically built for managing UAVs images, as Pix4UAV and AgiSoft Photoscan.

In the photogrammetric approach, exterior orientation parameters and ground point coordinates are estimated together with the related accuracies: however, some difficulties often arise during the image georeferencing and the block formation phase (bundle adjustment), especially when image positions and attitudes are far from those commonly obtained in a photogrammetric survey (aerial, terrestrial or close range).

On the other hand, by using software coming from CV, the processing of a large amount of images is usually faster and easier and digital model of the object, orthoimages and photorealistic 3D representations are produced with minor control on some processing steps (as georeferencing and block formation) and on the accuracies of computed geometric parameters.

Therefore, it is still necessary to test and compare the capabilities of different systems, in order to carefully assess the accuracies of final products and be aware in the choice of the system, which should be the most suitable for the survey purpose (Remondino et al. 2012).

Data acquisition

The area chosen for the test flight was a small rural area (roughly 30 hectares) located near Cisano Bergamasco (BG, Italy), belonging to the protected park 'Parco Adda Nord' in (Fruition of Goods Landscape in Interactive Environment—Gini et al. 2012). In this project aerial imagery acquired by UAVs is used to enhance the natural, artistic and cultural heritage, and to enhance the fruition of natural protected areas.

The area comprises some buildings, secondary roads, cultivated fields and natural vegetation (Fig. 1).

The employed UAV is a lightweight fixed wing SwingletCAM system produced by the Swiss company SenseFly (now part of the Parrot group), owned and operated by Studio di Ingegneria Terradat. This system is able to perform pre-planned flights in a fully automated mode; the SenseFly autopilot continuously analyzes data from the on-board GPS/IMU (Global Positioning System/inertial measurement unit) and takes care of all aspects of the flight mission: the SwingletCAM takes off, flies and lands fully autonomously.

Because of its very limited weight (<500 g) and size, autopilot smartness and ease of use, it is a suitable option to perform photogrammetric flights over limited areas at very high resolutions. The system incorporates a compact camera Canon Ixus 220HS (12 Mp and fixed focal length of 4.0 mm), capable of acquiring images with GSD (ground sample distance) of 3–7 cm, depending on the flight height.

Lombardy and already studied in the frame of FoGLIE project.

The average flight altitude was set at 132 m above ground level, variable between 130 and 135 m, in order to obtain a GSD equal to 4–5 cm, which is the optimized value for agricultural proximal sensing. Furthermore, in order to gain maximum stereoscopy and avoid holes, the flight planning was planned with longitudinal and lateral overlap equal to 80 %. Following this approach, seven strips would have been necessary to cover the area of interest; however, due to strong winds and turbulences in the area during the flight, the mission was aborted several times and a subsequent rearrangement of the flight plan limited the final acquisition to 5 strips and 49 images in total (Fig. 2). Despite this, the image overlap was always good even if lower than the planned one, in some portion of the block; a large number of homologous points can be identified contemporarily in many images (high multiplicity).

Despite the regular pattern of the flight planning, realized attitudes and positions of images resulted to have large differences, thus producing high variability in image scales and convergent images.

Approximate values for all the exterior orientation (EO) parameters were recorded during the flight by the SenseFly control system at each shot position.

For the block georeferencing and the subsequent accuracies analysis, 16 pre-signalized ground control points (GCPs) were distributed along the edges and in the middle of the area and their centre coordinates were measured by GPS (Trimble

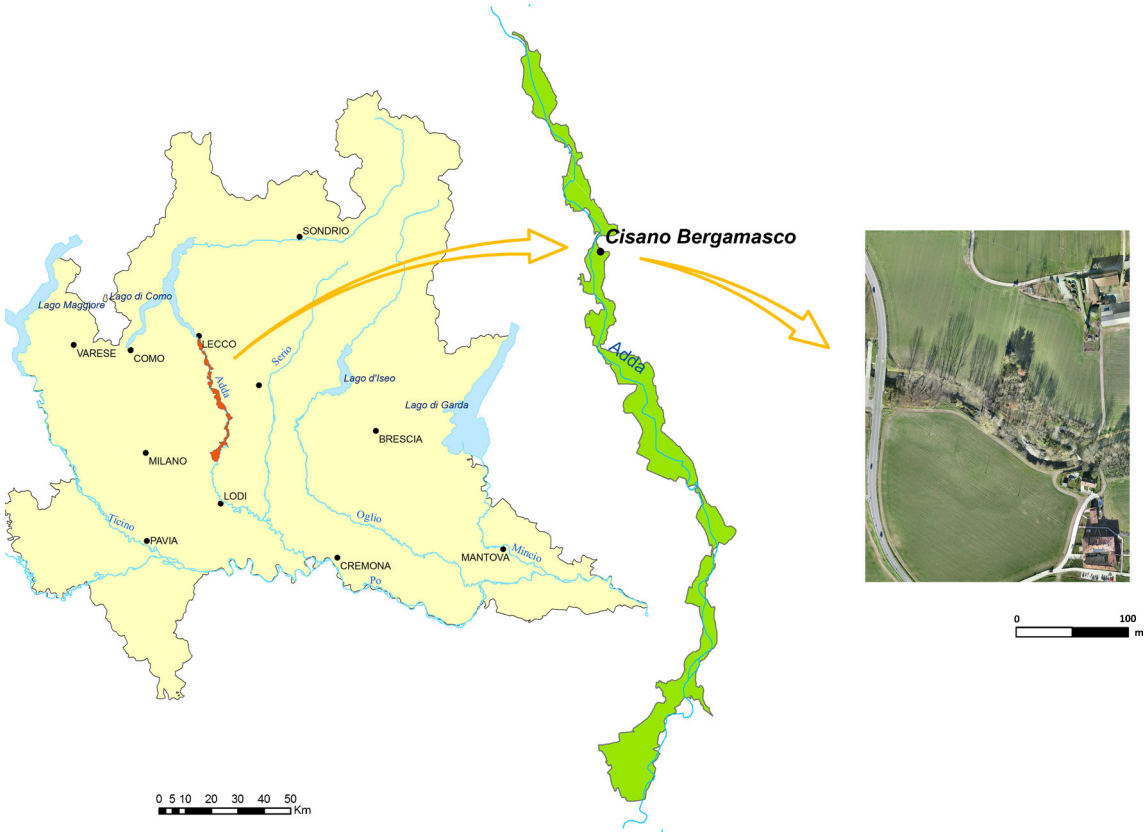

Fig. 1 Parco Adda Nord, in Lombardy and overview of the flown area near Cisano Bergamasco

5700) in NRTK (network real time kinematic) survey, with an accuracy of 2 cm horizontally and 5 cm in height. All the GCPs have been measured in UTM/ETRF2000 reference system. A subset of these were used as check points (CPs).

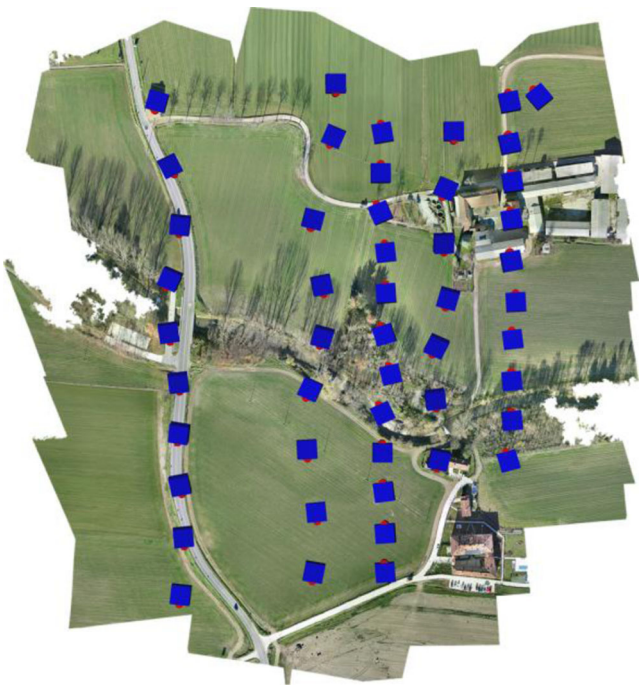

Fig. 2 Camera locations

Homologous point and feature extraction

As mentioned in the introduction, the images acquired with the SenseFly vector were processed using different software packages. The results were analysed both in terms of EO as well as in terms of traditional photogrammetric products (DSMs and orthophotos).

The employed software can be divided into two main categories: standard photogrammetric and computer vision software.

In the first group, software following a traditional workflow can be found: starting from the initial camera calibration step (Fraser 2013), then the GCPs identification and the tie point (TP) research, automatic or manual, in dependence on the specific tested program. After that, the images are oriented (with or without self-calibration refinement) and the subsequent DSM and orthophoto are realized.

In this context, Erdas Leica Photogrammetry Suite 2011(LPS), PhotoModeler Scanner V.7.2012.2.1 (from now on PM) and the scientific software EyeDEA were analyzed.

In the second group, 3D modelling software packages can be found: they carry out the image relative orientation together with the self-calibration, in an arbitrary reference system, which is often obtained using a minimum constraint coming from the approximate orientation provided by the UAV on board positioning system. Tie point extraction, measurement and outlier rejection are completely automatized steps (Barazzetti et al. 2010a, b; Pollefeys et al. 1999; Strecha et al. 2010); the subsequent use of GCPs allows to translate and rotate the photogrammetric block in a specific reference system. Pix4UAV Desktop (from now on P4) by Pix4D and Agisoft Photoscan (from now on APh) by AgiSoft LLC were taken under analysis.

A specific procedure was realized for each software package according to its characteristic, as briefly presented below.

LPS is a well-known photogrammetry system available in a user-friendly environment that guarantees photogrammetric precision. LPS provides tools for manual and automated measurement and for carrying out bundle adjustment computation, digital surface model generation, orthophoto production, mosaicking, and 3D feature extraction. With its tight integration with ERDAS Image software, LPS is a photogrammetric package for projects that involve various types of data and further processing and analyses of airborne imagery.

For this work TPs used to compute EO of the images were manually selected and measured, for a total of 295 points with an average multiplicity of 5 rays per point.

On the other hand, EyeDEA is a scientific software package developed by the University of Parma and it implements SURF (Speed Up Robust Feature) operator (Bay et al. 2008). Like any other interest operator (Remondino 2006), SURF allows one to identify a large number of matches with erroneous correspondence within each set: for this reason, EyeDEA implements also some robust error rejection techniques.

First of all, the fundamental matrix **F** (see Hartley and Zisserman 2006) is used to define the constraint between two sets of image coordinates: since the epipolar constraint is not sufficient to discriminate wrong matches between two points located on the epipolar line, also the trifocal tensor has been implemented. The RANSAC (RAndom SAmple Consensus) paradigm (Fischler and Bolles 1981) is run after each geometric control to guarantee a higher percentage of inlier. EyeDEA proceeds by successive image triplets, so the homologous points are seen, on average, only on three frames.

EyeDEA requires undistorted images as input, whose deformations were removed according to the models and parameters estimated with the camera calibration procedure implemented in the commercial software PM, making use of an ad hoc developed software, called 'DistRemover' (Univ. of Parma). As the number of TPs extracted with EyeDEA was too large (21224) and non-homogeneously distributed, it was decided to reduce them to better manage the photogrammetric block during the orientation phase as proposed in Barazzetti et al. (2010a). The point reduction was performed with an ad hoc developed Matlab® function, on the basis of the criteria of homogeneous distribution throughout the block and higher point multiplicity. In this way the final accuracy is not affected although the time required to compute the solution is significantly decreased; thus, the number of tie points was reduced to 2,924 image points.

Since the longitudinal overlap through the block was not always adequate to guarantee the automatic extraction of points on all the subsequent triplets and in order to strengthen the block itself, TPs extraction was also repeated along the transverse direction. Despite that, the software was not able at all to extract points on two images and for other six images it was necessary to manually measure some additional homologous points. Manual TP extraction was carried out with the commercial software PM in order to obtain the terrain coordinates necessary to the subsequent analysis and to manually measure the GCPs.

PhotoModeler Scanner allows users to accomplish fully automated projects (with the 'Smart Project' option), requiring as input only images and camera calibration parameters. It performs feature detection, image matching and orientation in a free-network mode. In a second phase user can add GCPs to constrain the block; PM can use a rigorous photogrammetric approach to minimize the block deformation throughout the bundle-block adjustment if one choose the 'control' option or can transform object coordinate without affecting the shape of the model itself (only by rotating, scaling and translating the model, like the most part of CV software does). For the present work the first procedure was applied, in order to obtain better quality result, similar to the one obtainable with a classic photogrammetric approach. During this step it is also possible to refine camera calibration parameters.

For what concerns the CV-based software, the specifically designed software for UAV application Pix4UAV was tested. It allows one to compute the block orientation in a fully automatic way, requiring as input only camera calibration parameters and an image approximate geo-location; moreover, GCPs were manually measured with the aim of comparing the results with the ones computed with other programs. The coordinates of all the points used to perform the bundle-block adjustment were exported and converted in the PM input format in order to generate the corresponding coordinates in the terrain reference system: these coordinates had to be used as approximate values for the next computations (see paragraph 4). The software allows users to create in an automatic way also the points cloud, the DSM and the orthophoto.

Eventually, APh was employed to automatically compute both image orientations and tie points cloud. It is a low cost commercial software, developed by Agisoft LCC, that allows to compute EO of large image datasets. First of all it performs a feature matching between the images, detecting points that are stable with respect to viewpoint and lighting variations.

These points are then used to generate a descriptor for each point based on its local neighbourhood. The descriptor is used in a second step to compute correspondence (with an approach similar to SIFT (Lowe 2004)). After this phase the software performs both interior and exterior orientation using a greedy algorithm to find approximate camera locations: then it refines their attitude using a classic bundle-block adjustment.

In this case the software extracted a large amount of points, so it was decided to decimate them considering only the points matched at least on three images, and that yield an RMSE (Root Mean Square Error) in the bundle adjustment lower than 0.40 m. The layouts of the TPs used in the four different software packages are shown in Fig. 3.

It is evident how the points extracted by using fully automated suites (such as PM and AS) outnumber the number of points extracted from other software packages. One can also notice how the points extracted by using PM Smart Projects are characterized, in average, by a greater number of rays per 3D point.

It is also interesting to notice how all the software packages that use feature based matching are unable to extract points more or less in the same areas, such as in correspondence of forest trees and fields with a particular homogenous texture. The result of EyeDEA is similar in terms of multiplicity, but the point set selected is smaller because the TPs were decimated before the bundle-block adjustment phase. P4 identified less points than APh but it was able to detect points visible on more images. The case of LPS is different because all the measurements were performed manually, by leading to an average multiplicity of five and a more uniform distribution.

Bundle-block adjustment

A standard procedure was defined to align the analysis of EO parameters, estimated by the different software: for this purpose the home-made scientific software Calge was used. Calge is a computer program designed to compute Least Squares adjustment of a general geodetic network or a photogrammetric block.

A first comparison between the different software packages involved the bundle-block adjustment using the TPs measured, either manually (LPS, some points for EyeDEA and all the GCPs) or automatically (the most of TPs extracted with EyeDEA and all the points identified by P4 and APh). In all cases, the calibration parameters were refined thank to the self-calibration executed during the bundle-block adjustment itself: especially, the variations of the 10 parameters of the model in Brown (1971) were estimated. The Canon Ixus 220HS optic is retractable to protect the lens during landing: for this reason is unavoidable to perform a self-calibration in order to estimate the correct interior orientation parameters.

For each software package, two different kinds of bundle-block adjustment were run: i) with constrains on all the measured GCPs; ii) with constrains only on 5 GCPs, 4 of which selected along the block edges and one near the center (see Fig. 4). Both GCPs and CPs measures on images were done manually by different non-expert operators.

In Table 1 the obtained results are listed.

The first columns show the number of TPs and the observation sample sizes: the ratio between these two quantities is equal to the average TPs multiplicity. In the subsequent column, the bundle-adjustment σ_0 is reported: it ranges from 0.3 μm (APh) to 2.6 μm (LPS), respectively 0.2 and 1.6 times the pixel size equal to 1.54 μm.

The estimated focal lengths, reported in the fifth row, varies between 4.234 mm (P4) and 4.438 mm (LPS), representing meaningful corrections with respect to the given initial value of 4.3559 mm that comes from the calibration procedure. On the other hand, the self-calibrated values do not vary significantly, also with respect to the estimated accuracies that are of the same order of magnitude. Moreover, as images were taken at constant height, there is a big correlation between estimated focal length (c) and estimated projection centers heights Z_0: a variation in c is absorbed by variation in Z_0.

In the following rows the RMS (Root Mean Square) of standard deviation of the TPs and RMSE (Root Mean Square Error) of the CPs are shown for each coordinate.

As expected, the RMS of the standard deviation values are smaller for software that extracted automatically a large number of TPs (also because of the lower value of σ_0). As regards LPS results, RMS high values are surely due to the small number of TPs, manually selected with high multiplicity, but not by expert photogrammetric technicians. Other software packages are almost fully automatic, so the extracted TPs number is higher and, consequently, the RMS of the standard deviation values are smaller (also because of the lower value of σ_0). As regards CPs RMSE, results are more homogenous, especially in east and north coordinates, for which they are around GSD whereas the differences are more pronounced in altitude. Especially, the best result has been obtained for APh (1.1*GSD both horizontally and in height) while the worst has been obtained for EyeDEA (respectively 2.2*GSD horizontally and 4.3*GSD for height coordinates).

A further analysis was carried out with Calge, in order to evaluate the quality of EO parameters estimated by each software. Exterior orientations obtained by different software packages by using the 5 selected GCP (Fig. 4) were used as fixed constrains in Calge to estimate CP coordinates. Since EyeDEA performed only the TPs extraction, the EO parameters were calculated by PM. At the same time also a self-calibration was performed, in order to evaluate the best

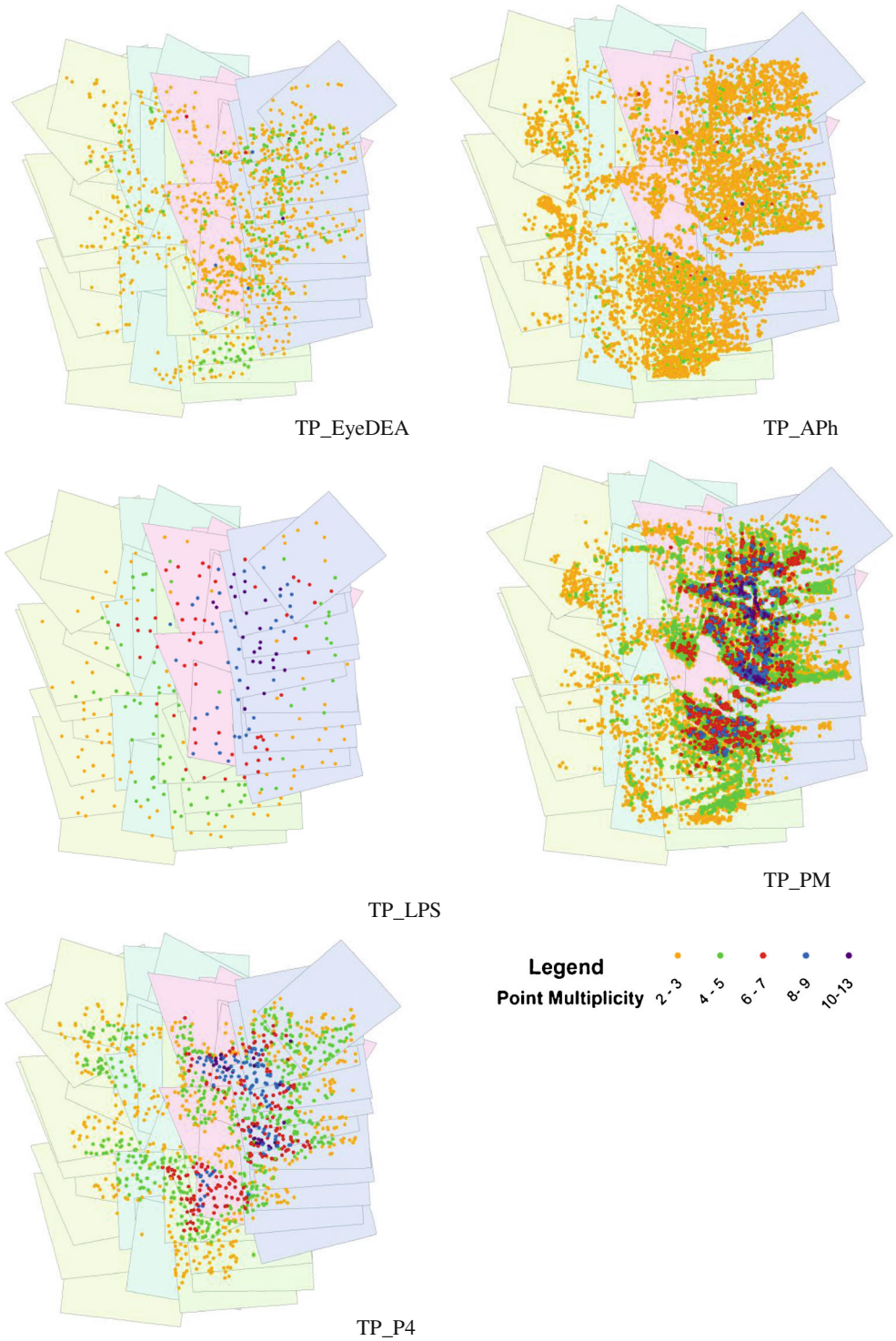

Fig. 3 Tie points distribution on the images for the different software: from top to bottom LPS, EyeDEA, P4, APh, PM

calibration parameters set. The RMSE of CPs residuals are summarized in Table 2.

The RMSE values are low with respect to the image scale of 1:31,000 and the GSD equal to 4.5 cm. Considering the horizontal coordinates, the minimum value (0.33*GSD) was achieved with the combination of the software PM and EyeDEA, followed by LPS (1*GSD). Worse results were obtained by P4 and APh.

When height coordinates are considered, the RMSE are higher than horizontal ones, even if the values are smaller than 100 mm (with the exception of the value obtained by processing the block with P4, which is equal to 214 mm).

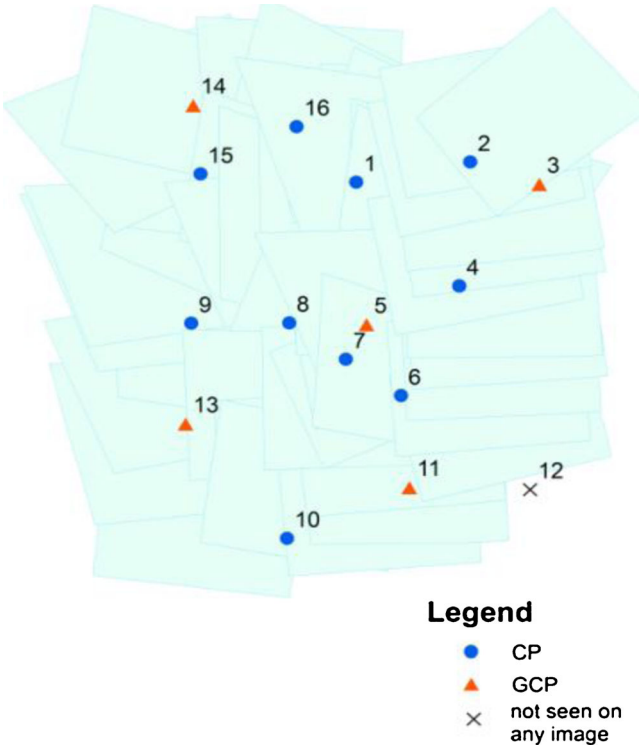

Fig. 4 The 10 CPs employed in the analysis with 5 GCPs

DSM comparisons

A second kind of comparison among software results was done analyzing the DSM produced. A mesh of 0.20 m was chosen to compute surface models with different software packages. Automatic procedures were used to produce directly the DSM in LPS, P4 and APh whilst PM was used to produce a point cloud as well as another home-made software called Dense Matcher (DM—Re et al. 2012), used to process the data coming from EyeDEA/PM workflow. The points cloud created by PM and DM were interpolated on the same grid mesh through ArcGIS 10.0. A first visual analysis (see Fig. 5) shows that not all the software can create DSM in the whole area: especially the one made with DM is characterized by some gaps located in those areas where the number of overlapping images is low and the texture is poor.

A different behavior can be observed also where sharp height variations occur, for instance around buildings. P4, DM, LPS and PM indeed compute interpolated values, as in all the other parts, while APh, run in 'sharp' mode, seems to recognize edges and produces a sharper DSM.

This is clearly visible in the layouts where the differences coming from APh and the other software packages are presented (see Fig. 6).

Statistics of the differences are shown in Table 3.

The average value is of some centimeters for the all differences while the standard deviation is approx. 1 m for P4-APh,

Table 2 RMSE on the CPs residuals obtained in the second test (fixed EO)

	LPS	EyeDEA/PM	P4	APh	PM
E [mm]	48	16	81	74	51
N [mm]	47	12	46	61	41
h [mm]	90	36	214	83	137

Table 1 Bundle-block adjustment results (15 and 5 GCPs configuration)

Software TPs' generator	# TPs	# observed points	# GCPs	σ_0	Theoretical Accuracy (RMS of std.dev.) of TPs			Empirical accuracy (RMSE) of CPs			Estimated focal lenght	# rays per point
				[μm]	Est [mm]	Nord [mm]	h [mm]	Est [mm]	Nord [mm]	h [mm]	[mm]	
LPS[a]	285	1492	15	2.6	109	89	215	–	–	–	4.437	5
			5	2.6	119	101	259	50	50	130	4.438	5
EyeDEA[b]	1052	3395	15	1.4	57	50	142	–	–	–	4.295	3
			5	1.4	68	61	181	73	81	329	4.295	3
PM	13647	55887	15	1.1	23	21	57	–	–	–	4.389	4
			5	1.1	26	23	66	54	50	114	4.390	4
Pix4UAV	1317	6146	15	1.0	25	23	61	–	–	–	4.234	5
			5	1.0	30	28	76	39	54	213	4.237	5
Agisoft PhotoScan	6098	19097	15	0.3	8	7	20	–	–	–	4.361	3
			5	0.3	9	8	23	50	19	55	4.360	3

[a] Manual measurements

[b] Some manual measurements

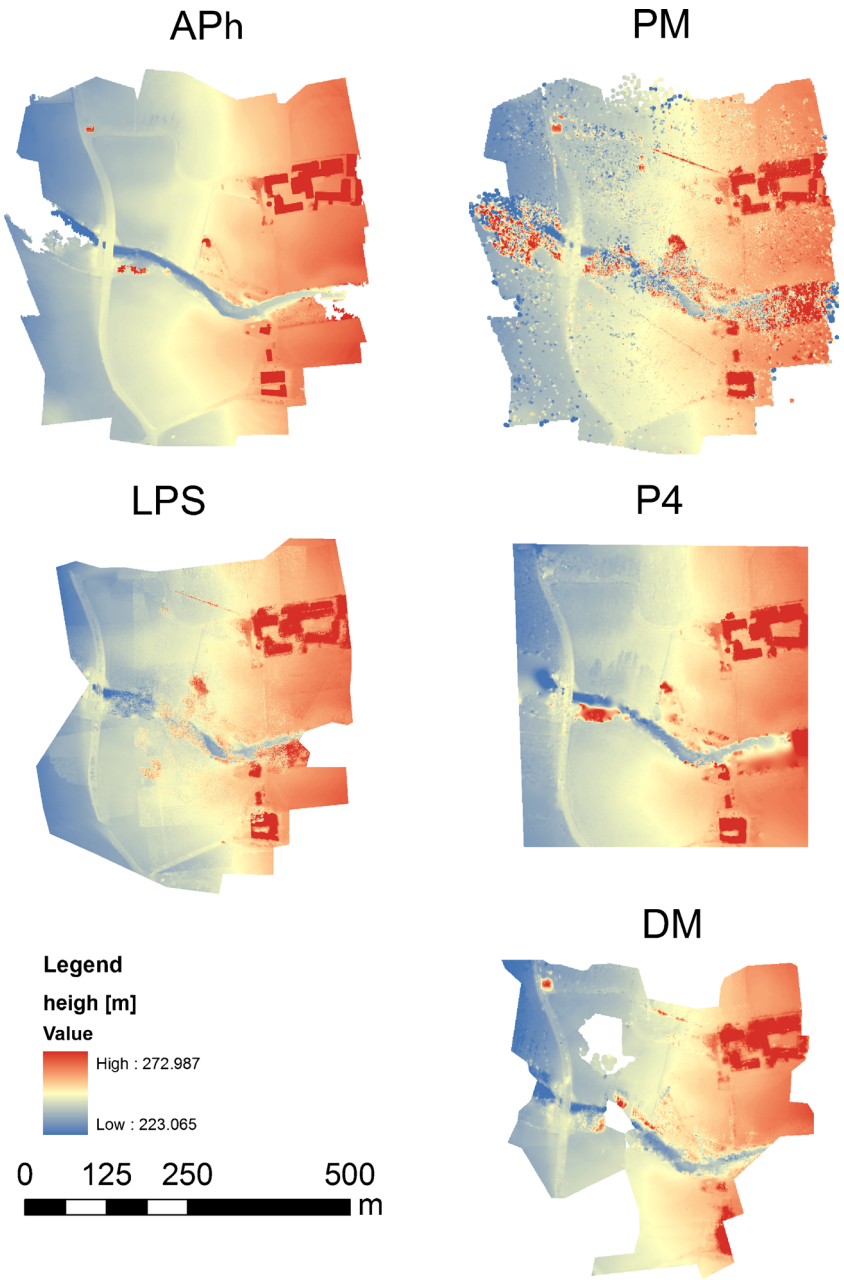

Fig. 5 DSM from APh, LPS, P4 and DM

DM-APh and LPS-APh differences; a bit more noisy is the difference of PM-APh. The maximum absolute values are about 20 m near building edges and in the central area covered by very high trees.

In most areas (about 90 %) differences are in the range from −0.3 to 0.4 m. The average of the differences close to zero shows the absence of vertical and horizontal biases for all DSMs.

A detailed analysis made on a regular and flat area (green square in Fig. 7) has been performed. Because of some visible jumps present in PM and LPS DSMs along some image borders, the comparisons are presented only for the other software packages (APh, P4 and DM).

In Table 4 statistics of the differences with respect to APh are illustrated.

Mean and standard deviation values are moderate for both the comparisons. In Fig. 7 the analysis done with ArcGIS are shown. The different smoothing effects generated by various surface reconstruction approaches are confirmed (see Fig. 7).

In P4-APh comparison, the anomalous behavior visible in the red circle is due to the presence of tree shadows (see Fig. 8): the almost flat ground was modeled in one case with

Fig. 6 DSM differences

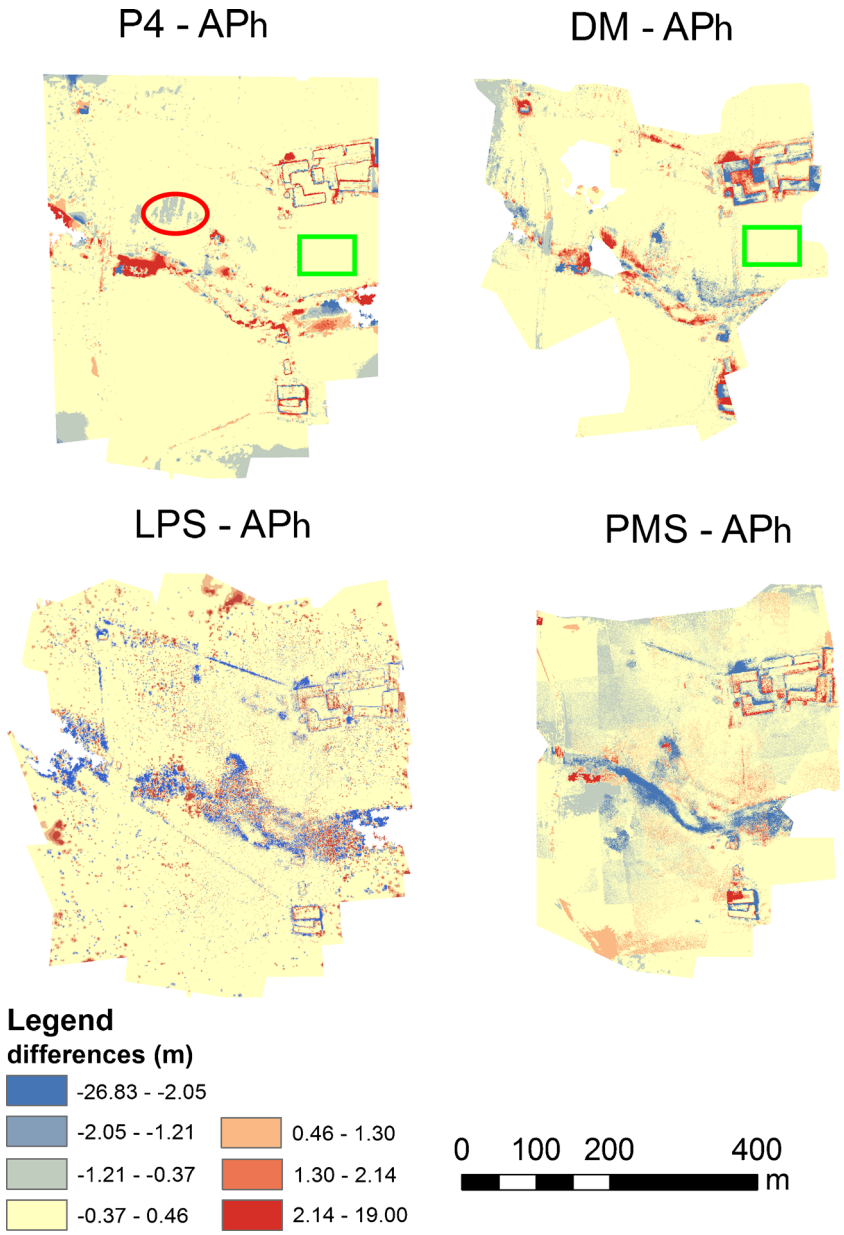

false height variations of the order of 1 m. This is probably due to homologous points chosen at shadow edges, which are slightly moving during the survey, thus causing mismatching and false intersections. This effect is visible also in the LPS and DM DSMs. Again, there is a different software behavior: P4 and the other software packages produced higher and sharper undulations, while APh gave a smoother surface.

Finally, Fig. 9 shows the two orthophotos carried out from the DSM generated by P4 (above) and APh (below) with a resolution of 20 cm. The different behaviour near the roof edges is clear: APh defined the edges better than P4.

Table 3 Statistics of DSM differences

	Mean [m]	St.dev. [m]	Min [m]	Max [m]
P4-APh	0.06	0.84	−11.11	19.00
DM-APh	−0.01	0.89	−15.30	16.03
LPS-APh	−0.12	1.03	−15.73	15.19
PM-APh	0.06	1.57	−26.83	17.85

Conclusions

The rapid dissemination of UAV systems and computer vision software opens new application scenarios in the context of the

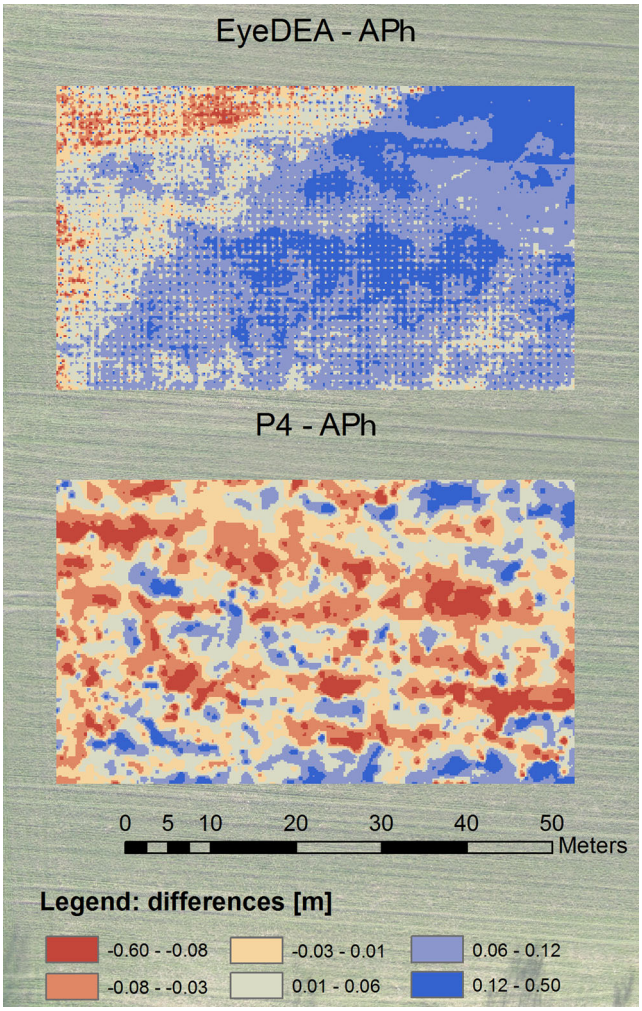

Fig. 7 Differences of DSMs: detail in flat area

land management. In this work a survey of heritage landscape was carried out for environmental documentation and monitoring purposes, with an UAV. The images acquired by UAVs (in particular the fixed-wing ones), are suitable to be processed by different software packages developed in both computer vision and photogrammetric communities (even home-made like EyeDEA and Dense Matcher). All software packages were able to provide the exterior orientation of the images and products such as the digital surface model (DSM). Programs of the first type can work almost entirely in an automatic way and they can quickly create a high quality final product. Moreover, Pix4UAV, PhotoModeler Scanner and

Table 4 Statistics of DSM difference in the flat region

	Mean [m]	St.dev. [m]	Min [m]	Max [m]
P4-APh	0.00	0.07	−0.37	0.49
DM-APh	0.08	0.06	−0.54	0.39

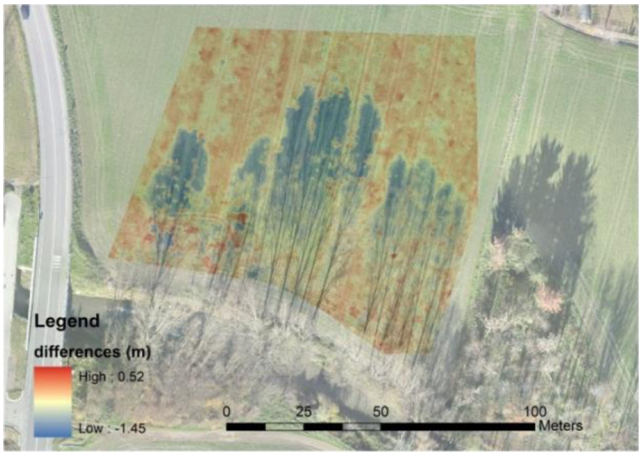

Fig. 8 Differences of DSMs (P4-APh): detail in shadow area produced from trees

Agistoft Photoscan can automatically generate very dense point clouds with high multiplicity.

The photogrammetric software requires an operator's intervention in some phases, as in the exterior orientation validation, in the estimation of the self-calibration parameters or in the manual selection of points in critical areas of the images. The computational time is often very high in comparison with the other software packages. For instance, the DSM generation in Dense Matcher required many hours of processing. On the other hand, the photogrammetric software results are better

Fig. 9 Differences of ortophotos (APh up—P4 down): detail in the edges of some buildings

(see Table 2), in terms RMSE of control points obtained by constraining the exterior orientation parameters. The results obtained in terms of DSM and orthophoto during the tests with Agisoft Photoscan seem to achieve the most reliable results; this is highlighted by a comparison of details rather than a global analysis (indeed, all products did not have systematic errors). Moreover, Agisoft Photoscan provided the best product, especially in flat areas and in the presence of shadows. Eventually, the strategy that this software package employs for the buildings outlines allows the creation of orthophotos with a high level of quality (see Fig. 9).

Acknowledgments The authors would like to thank Dr Riccardo Roncella for providing the software EyeDEA and Terradat company, owned by Paolo Dosso, who performed the flight with SenseFly System. The project has been sponsored by Regione Lombardia (Italy)

References

Barazzetti L, Remondino F, Scaioni M, Brumana R (2010a) Fully automatic UAV image-based sensor orientation. Int Arch Photogramm Remote Sens Spatial Inf Sci XXXVIII(1):6

Barazzetti L, Scaioni M, Remondino F (2010b) Orientation and 3D modeling from markerless terrestrial images: combining accuracy with automation. Photogramm Rec 25(132):356–381

Bay H, Ess A, Tuylelaars T, Van Gool (2008) Speeded Robust Features (SURF). Comput Vis Image Underst 110:346–359

Brown DC (1971) Close-range camera calibration. Photogramm Eng 37(8):855–866

Colomina I, Blazquez M, Molina P, Parés ME, Wis M (2008) Towards a new paradigm for high-resolution low-cost photogrammetry and remote sensing. IAPRS SIS 37(B1):1201–1206

Eisenbeiss H, Sauerbier M (2011) Investigation of UAV systems and flight modes for photogrammetric applications. Photogramm Rec 26(136):400–421

Fischler M, Bolles R (1981) Random sample consensus: a paradigm for model fitting with application to image analysis and automated cartography. Commun Assoc Comp Mach 24:81–95

Forlani G (1986) Sperimentazione del nuovo programma CALGE dell'ITM. Boll SIFET 2:63–72

Fraser CS (2013) Automatic camera calibration in close range photogrammetry. Photogramm Eng Remote Sens 79:381–388

Gini R, Passoni D, Pinto L, Sona G (2012) Aerial images from an UAV system: 3d modeling and tree species classification in a park area. Int Arch Photogramm Remote Sens Spatial Inf Sci XXXIX-B1:361–366

Grenzdörffer GJ, Engel A, Teichert B (2008) The photogrammetric potential of low-cost UAVs in forestry and agriculture. IAPRS SIS 37(B1):1207–1213

Haarbrink RB, Koers E (2006) Helicopter UAV for photogrammetry and rapid response. In: International Archives of Photogrammetry, Remote Sensing and Spatial Information Sciences, ISPRS Workshop of Inter-Commission WG I/V, Autonomous Navigation, Antwerp, Belgium

Hartley R, Zisserman A (2006) Multiple view geometry in computer vision. Cambridge University Press, UK

Lowe DG (2004) Distinctive image feature from scale-invariant key points. Int J Comput Vis 60(2):91–110

Pollefeys M, Koch R, Van Gool L (1999) Self-calibration and metric reconstruction inspite of varying and unknown internal camera parameters. IJCV 32(1):7–25

Re C, Roncella R, Forlani G, Cremonese G, Naletto G (2012) Evaluation of area-based image matching applied to DTM generation with Hirise images. ISPRS Ann Photogramm Remote Sens Spatial Inf Sci I-4:209–214

Remondino F, Del Pizzo S, Kersten T, Troisi S (2012) Low-cost and open-source solutions for automated image orientation—a critical overview. Progress in Culturale Heritage Preservation. Lecture Notes in Computer Science. Vol.7616, pp 40–54

Remondino F, Gruen A, von Schwerin J, Eisenbeiss H, Rizzi A, Giraldi S, Sauerbier M, Richards-Rissetto H (2009) Multi-sensor 3D documentation of the Maya site of Copan. Proceedings of the XXIInd CIPA Symposium

Remondino F, Barazzetti L, Nex F, Scaioni M, Sarazzi D (2011) UAV photogrammetry for mapping and 3D modeling—current status and future perspectives. Int Arch Photogramm Remote Sens Spat Inf Sci XXXVIII-1/C22:25–31. doi:10.5194/isprsarchives-XXXVIII-1-C22-25-2011

Remondino F (2006) Detectors and descriptors for photogrammetric applications. Int Arch Photogramm Remote Sens Spat Inf Sci 36(3):4914

Roncella R, Re C, Forlani G (2011) Performance evaluation of a structure and motion strategy in architecture and cultural heritage. Int Arch Photogramm Remote Sens Spatial Inf Sci XXXVIII-5(W16):285–292

Strecha C, Pylvanainen T, Fua P (2010) Dynamic and scalable large scale image reconstruction. Comput Vis Pattern Recognit (CVPR), IEEE Conference on, pp. 406–413